Effect of Arginine on Protein Aggregation Studied by Fluorescence Correlation Spectroscopy and Other Biophysical Methods[†]

Ranendu Ghosh,[‡] Sunny Sharma,[‡] and Krishnananda Chattopadhyay*

Structural Biology and Bioinformatics, Indian Institute of Chemical Biology, Council of Scientific and Industrial Research, 4, Raja S. C. Mullick Road, Kolkata 700032, India

Received November 7, 2008; Revised Manuscript Received December 8, 2008

ABSTRACT: Arginine has been used extensively as an excipient in the formulation development of protein-based biopharmaceuticals. We investigate the role of arginine in suppressing protein aggregation and its mechanism by using bovine serum albumin as a model system. By using sedimentation velocity and other analytical techniques, we show that the use of arginine inhibits temperature-induced aggregation of the protein. We use fluorescence correlation spectroscopy and other spectroscopic techniques to show that arginine inhibits accumulation of partially folded intermediates, potentially involved in the aggregation process. The hydrodynamic radii of the protein in its native, unfolded, and intermediate states have been determined using fluorescence correlation spectroscopy at single-molecule resolution. A possible mechanism of the effects of arginine and its role as an aggregation suppressor has been discussed.

Protein aggregation poses major problems in the development of recombinant protein-based biopharmaceuticals. Aggregates are often immunogenic and hence undesirable in manufacturing and formulation development (*1, 2*). Additionally, aggregation leads to precipitation of active compounds resulting in loss of ingredients as well as an increase in material costs. Arginine has been used extensively to improve refolding yield and to suppress aggregation in a number of recombinant protein systems (*3*−*5*). Addition of a high concentration of arginine has been shown to improve the recovery of antibody molecules from protein A columns (*3, 6*). While the use of arginine in the manufacturing and formulation of therapeutics has been growing, the mechanism of its action is still unknown. It has been shown previously that arginine may be different from other amino acids like glycine or proline by virtue of its protein perturbing nature (*7*). Baynes et al. recently suggested that arginine inhibits aggregation by slowing protein−protein interaction and its role can be predicted by gap effect theory (*8*). Gap effect theory suggests that solution additives like arginine, which is much larger than water, increase the activation energy of protein−protein association without changing the free energy of isolated protein molecules (*8*).

Guanidine hydrochloride is a known protein-denaturing agent. Arginine also contains a complex guanidinium group in its chemical structure. It has been suggested that arginine, by virtue of its structural similarity with guanidine hydrochloride, may have a protein destabilizing role (*7, 9*). It has been shown recently that arginine has weak binding affinity toward the aromatic region of a protein (*3*).

Fluorescence correlation spectroscopy (FCS)[1] is emerging as an important technique in modern biochemistry and biophysics for studying diffusional and conformational properties of labeled biomolecules at single-molecule resolution (*10*−*13*). FCS measures fluorescence fluctuations in a small observation volume while the system is kept under thermodynamic equilibrium. These fluctuations can originate either from the molecular diffusion inside the observation volume or through any chemical kinetics or conformational events. It has been shown recently that FCS can be used to detect protein folding intermediates in the unfolding pathway of intestinal fatty acid binding protein (*14, 15*). The conformational dynamics of the fatty acid binding protein in its folded and unfolded states have also been monitored by FCS (*16*). The application of FCS has been extended to study protein aggregation and protein−protein interactions both in solution and in a cellular environment (*17*−*21*).

In this work, we used FCS in conjunction with other biophysical techniques to study the effect of arginine on protein aggregation using bovine serum albumin (BSA) as a model protein. We chose BSA for our study because it plays key roles in the transport of a large number of commonly used drugs. Additionally, the conformational properties and aggregation of BSA have been extensively studied (*22*−*25*). We show using a number of analytical techniques, including sedimentation velocity, dynamic light scattering, and gel electrophoresis, that the heat-induced aggregation of BSA is inhibited by addition of arginine. To understand the roles of arginine in protein stability and conformation, we have studied unfolding transitions of BSA using a number of techniques, including far-UV circular dichroism (CD), steady state fluorescence, and FCS. By using FCS, we have calculated the hydrodynamic radii of BSA in its native, unfolded, and intermediate states. We show that

[†] Funded by CSIR Network Project Grant NWP005, CSIR, India.

* To whom correspondence should be addressed. Telephone: 91-33-2473-0492. Fax: 91-33-2473-5197. E-mail: krish@iicb.res.in.

[‡] These authors contributed equally to this work.

[1] Abbreviations: FCS, fluorescence correlation spectroscopy; CD, circular dichroism; BSA, bovine serum albumin; MEM, maximum entropy method; APD, avalanche photodiodes; ASA, accessible solvent area.

10.1021/bi802065j CCC: $40.75
Published on Web 01/15/2009

arginine inhibits the formation of partially folded intermediates in the unfolding transitions of BSA which may have direct relevance with respect to its ability to block protein aggregations.

MATERIALS AND METHODS

Protein Sample and Reagents. BSA (A7638) was obtained from Sigma Chemical Co. (St. Louis, MO). Urea and acrylamide were obtained from Sigma-Aldrich at the highest available grade. Alexa488Maleimide was obtained from Molecular Probes (Eugene, OR). DL-Arginine (for CD experiments) was obtained from MP Biomedical. All other reagents used were high-grade analytical reagents. For tryptophan fluorescence and CD experiments, 20 mM sodium phosphate buffer (pH 7.5) was used, and for sedimentation velocity experiments, phosphate-buffered saline (PBS) buffer (pH 7.4) was used.

Sedimentation velocity experiments were performed using a Beckman Optima XL-I analytical ultracentrifuge at 20 °C using an An-50 Ti rotor. To avoid any suspended particle, protein samples as well as the reference buffer solutions were centrifuged at 5000 rpm for 4 min at room temperature in a tabletop centrifuge (Tarson) immediately before the experiments. Aggregated protein samples of 400 μL were loaded against 420 μL of equivalent buffer as a reference into 12 mm charcoal-filled Epon centerpieces and centrifuged at 42000 rpm for 8 h. Sedimentation velocity data were analyzed with SEDFIT using the continuous $c(s)$ distribution model (*26*). Collections of the first 55 scans were used for the analysis with s values between 2 and 40. The positions of the cell bottom and meniscus were determined manually and then refined in the final fit.

CD spectra were recorded using a Jasco J715 spectropolarimeter (Japan Spectroscopic Ltd.). Far-UV CD measurements (between 200 and 250 nm) were performed with 1 μM protein using a cuvette with a path length of 1 mm. Ten spectra were collected in continuous mode and averaged. For near-UV CD experiments (between 250 and 350 nm), ~10 μM protein was used in a cuvette with a path length of 1 cm. Three spectra were recorded in continuous mode and averaged.

Dynamic light scattering experiments were performed at 25 °C using a Nano-ZS (Malvern Instruments) instrument (5 mW, He−Ne laser, $\lambda = 632$ nm). The operating procedure was programmed (using the DTS software supplied with the instrument) to record the average of 10 runs, each run being collected for 30 s with an equilibration time of 3 min.

Steady state fluorescence experiments were performed with 1 μM protein samples using a Hitachi F4500 spectrofluorometer. The samples were excited at 295 nm to avoid contributions from tyrosine residues. While emission wavelengths were scanned between 310 and 450 nm, the emission intensity at 340 nm was typically plotted for the unfolding experiments. Necessary inner filter effect corrections were performed using reported methods (*27*).

FCS Experiments with Labeled BSA. Labeling of BSA with Alexa488Maleimide was carried out using a published procedure (*14*). A solution of Alexa488Maleimide in DMSO was slowly added to a 1 mg/mL solution of BSA with constant stirring. The molar ratio of the dye and the protein was kept at 10:1. The resulting solution was incubated for 5 h at 4 °C with shaking after every 30 min, after which the reaction was quenched by addition of excess β-mercaptoethanol. The excess free dye was removed by extensive dialysis followed by column chromatography using a Sephadex G20 column equilibrated with 20 mM sodium phosphate buffer (pH 7.5). The extent of labeling was calculated to be approximately 68%.

FCS experiments were carried out using a commercial instrument, confocor 3 LSM (Carl Zeiss, Evotec, Jena, Germany), using a 40× water immersion objective. Approximately 500 μL of the sample (dye or labeled protein) was placed into Nunc chambers (Nalge Nunc) and excited with an argon laser at 488 nm. The fluorescence signal was separated from the excited line using a main dichroic filter and collected using avalanche photodiodes (APD). The photocurrent detected by the APD was used by the correlator to calculate the correlation function.

FCS experiments were conducted in 20 mM sodium phosphate buffer (pH 7.5). Typically, 50−100 nM labeled protein was used. Excess unlabeled BSA was added to Nunc chambers before FCS experiments to minimize surface adsorption of the labeled protein samples. To correct for the refractive index and viscosity of the urea and arginine solutions, necessary correction measures were taken using a microscope correction collar and height as described previously (*15*). Moreover, FCS experiments were carried out with a free fluorophore (Alexa488Maleimide) under each solution condition to normalize the protein data (*17*).

Analysis of the Correlation Functions Using a Conventional Method. For a single-component system, the diffusion time (τ_D) of a fluorophore and the number of particles (N) can be calculated by fitting the correlation function [$G(\tau)$] to eq 1:

$$G(\tau) = 1 + \frac{1}{N}\left(\frac{1}{1+\frac{\tau}{\tau_D}}\right)\left(\frac{1}{1+S^2\frac{\tau}{\tau_D}}\right)^{0.5} \quad (1)$$

where N is the number of particles in the observation volume and S is the structure parameter, which is the depth to diameter ratio of the Gaussian observation volume.

The diffusion coefficient (D) of the molecule can be calculated from τ_D using eq 2:

$$\tau_D = \frac{\omega^2}{4D} \quad (2)$$

where ω is the beam radius of the observation volume, which can be obtained by measuring the τ_D of a fluorophore with a known D.

The hydrodynamic radius (r_H) of a labeled molecule can be calculated from D using the Stokes−Einstein equation (eq 3):

$$D = \frac{kT}{6\pi\eta r_H} \quad (3)$$

where k is the Boltzmann constant, T is the temperature, and η corresponds to the viscosity of the solution.

Data Analysis Using the Maximum Entropy Method (MEM). The correlation function data were further analyzed by the maximum entropy method recently applied to FCS using the MEMFCS algorithm (*28*). In this method, the multicomponent correlation function can be represented by eq 4 as

$$G(\tau) = \sum_{i=1}^{n} a_i \left(\frac{1}{1+\frac{\tau}{\tau_{D_i}}}\right)\left(\frac{1}{1+S^2\frac{\tau}{\tau_{D_i}}}\right)^{0.5} \quad (4)$$

where n is the number of noninteracting fluorescent species each of which can have a diffusion time between 0.001 and 500 ms. MEMFCS maximizes an entropic quantity $S = \sum_i p_i \ln p_i$ to yield an optimized fit.

Equilibrium Unfolding Transition. Protein samples in 20 mM sodium phosphate buffer (pH 7.5) were incubated with different concentrations of urea overnight at room temperature. The samples were analyzed using different spectroscopic techniques like steady state fluorescence, CD, or FCS. Far-UV CD data were fit to a simple two-state unfolding transition using eq 5:

$$\theta = \{\theta_N + m_N[\text{urea}] + (\theta_D + m_D[\text{urea}])\exp[-(\Delta G^\circ + m[\text{urea}]/0.58263)]\}/\{1+\exp[-(\Delta G^\circ + m[\text{urea}]/0.58263)]\} \quad (5)$$

where θ is the observed ellipticity, θ_N and θ_D are the ellipiticity values for the native and completely unfolded proteins, respectively, extrapolated to zero urea concentration, ΔG° is the free energy of unfolding, and m corresponds to the cooperativity of unfolding transition.

Data Analysis. All the data were analyzed and fit by using OriginPro version 7.5 (OriginLab Corp.).

RESULTS

Heat-Induced Aggregation of BSA and Effects of Arginine. Aggregation of BSA was induced by incubating the protein at 80 °C for 15 min, and the resulting solutions were studied by sedimentation velocity, dynamic light scattering, and native gel electrophoresis. Figure 1a shows the continuous $c(s)$ distribution of heat-treated BSA as obtained by SEDFIT analysis of sedimentation velocity data. The representative residual distribution of the fit is also shown, and the randomness of the residual distribution shows the goodness of the fit. The continuous $c(s)$ distribution indicates the presence of a number of different components, including BSA monomer (sedimentation coefficient of 5), dimer (sedimentation coefficient of 7.5), and larger aggregates with unresolved sedimentation coefficients. Figure 1b shows the variation of the percentage of BSA monomer with arginine concentration (■). The data show a significant increase in the monomer percentage. The heat-induced aggregation of BSA in the presence of arginine was further investigated by measuring the average radius using dynamic light scattering. Figure 1b shows the values of the average radii of heat-treated BSA in the presence of 0, 100, and 500 mM arginine obtained by dynamic light scattering (□). A systematic decrease in the values of the average radius in the presence of arginine provides further evidence that arginine inhibits BSA aggregation. Figure 1c summarizes the results of native gel electrophoresis analysis of heat-treated BSA samples, which clearly shows the increase in the magnitude of the monomer band with the increase in arginine concentrations and subsequent decrease in the extent of BSA aggregation in the presence of arginine.

Secondary and Tertiary Structure of BSA in the Presence of Arginine Monitored by Circular Dichroism (CD). Far-UV CD (between 200 and 250 nm) is routinely used to monitor any changes in the secondary structure of a protein. Near-UV CD, on the other hand, is used to probe tertiary structure. Far- and near-UV CD spectra of BSA in the presence of 0 and 500 mM arginine are shown in panels a and b of Figure 2, respectively. Far-UV CD data show that addition of arginine did not change the secondary structure of the protein (Figure 2a). However, far-UV CD data below 215 nm are unreliable as a result of the high sample

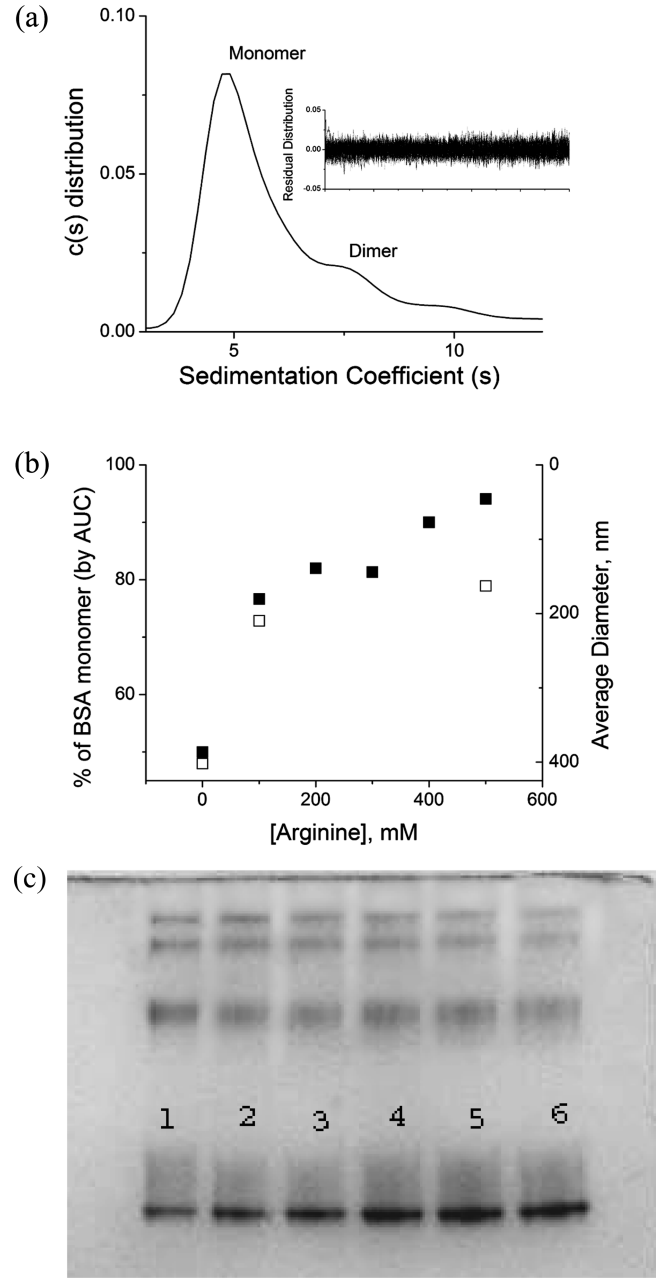

FIGURE 1: (a) Continuous $c(s)$ distribution of heat-treated BSA in the presence of 20 mM sodium phosphate buffer (pH 7.5). The positions of the monomer and dimer are shown. The residual distribution of the fit obtained by SEDFIT analysis is shown in the inset. (b) Effect of arginine concentration on the monomer percentage [(■) sedimentation velocity data] and the average diameter [(□) dynamic light scattering data]. (c) Native gel electrophoresis analysis of the heat-treated BSA samples in the presence of different concentrations of arginine. Lane 1 contained heat-treated BSA without arginine. Lanes 2−6 contained heat-treated BSA samples with increasing concentrations of arginine: 100, 200, 300, 400, and 500 mM, respectively. Heat-treated samples were prepared by heating BSA samples in the presence of different concentrations of arginine to 80 °C for 15 min at pH 7.5.

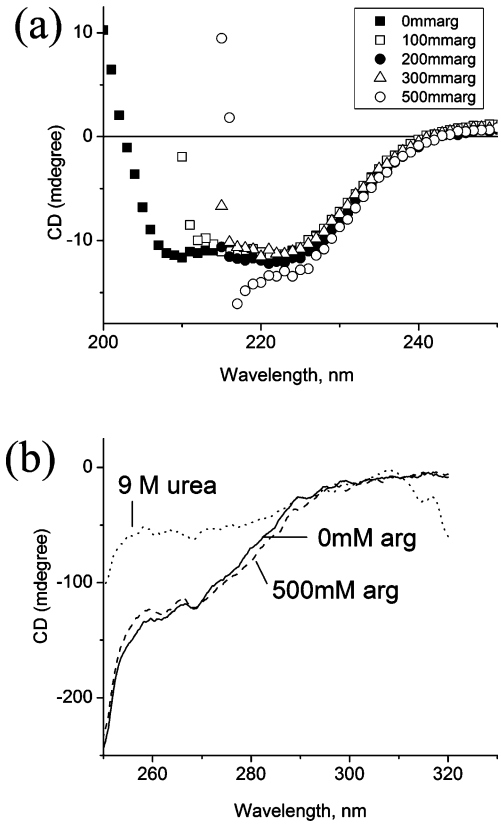

FIGURE 2: Effect of arginine on BSA monitored by (a) far-UV and (b) near-UV CD. Experiments were performed in 20 mM sodium phosphate buffer (pH 7.5) at room temperature.

absorbance, particularly in the presence of high concentrations of arginine. Near-UV CD, on the other hand, shows a small difference around 280 nm, suggesting possible interaction of arginine with the aromatic amino acids of the protein. While the change in near-UV CD is small and somewhat inconclusive, independent reports confirm the interactions of arginine with aromatic residues of a protein (*3*).

Effects of Arginine on the Urea-Induced Equilibrium Unfolding Transitions of BSA Monitored by Steady State Fluorescence and Far-UV CD. To understand the effect of arginine on conformational stability, steady state fluorescence and far-UV CD were used to monitor the unfolding transitions of BSA in the absence and presence of different concentrations of arginine at room temperature. Changes in the steady state fluorescence provide information about the changes in the local environment of tryptophan residues. The decrease in CD at 222 nm with urea concentration corresponds to the unfolding of the secondary structure of an α-helical protein.

Figure 3a shows the unfolding transitions of BSA in the presence of 0, 100, 200, 300, and 500 mM arginine monitored by steady state fluorescence monitored at 340 nm. Figure 3b shows the corresponding unfolding transitions probed by far-UV CD. Steady state fluorescence measurements (Figure 3a), which monitor the local environment of the tryptophan residues, suggest deviation from two-state behaviors in the presence of 0, 100, and 200 mM arginine. Over this range of arginine concentrations, urea-induced unfolding of BSA probed by tryptophan fluorescence has at least two steps. The first step occurs at a low urea concentration accompanied by a significant increase in the steady state fluorescence intensity. This is then followed by a second step with a large decrease in fluorescence intensity. Unfolding of the secondary structure of BSA monitored by far-UV CD (Figure 3b), on the other hand, is a typical two-state transition for each arginine concentration. Far-UV CD at 222 nm did not exhibit any intermediate or pretransition baseline change either in the absence or in the presence of arginine.

A comparison between the unfolding transitions probed by steady state fluorescence and by far-UV CD for BSA in the absence of arginine is shown in Figure 3c, which shows a large difference presumably because of the presence of the intermediate. For example, at 4.5 M urea, a large change (more than 50%) in the tryptophan fluorescence has been observed while the change in far-UV CD is insignificant (Figure 3c). This suggests that the unfolding of the local environment of tryptophan (steady state fluorescence) and the unfolding of the secondary structure (far-UV CD) do not occur simultaneously in the absence of arginine because of the formation of an intermediate. The secondary structure of the intermediate is intact, while its tryptophan environment must be significantly perturbed. Figure 3d shows the corresponding unfolding data in the presence of 500 mM arginine which can be superimposed with each other. In the presence of 500 mM arginine, unfolding of the local tryptophan environment and the global unfolding occur simultaneously, and no intermediate has been detected by steady state fluorescence or far-UV CD.

The unfolding transitions of the secondary structure of BSA (probed by far-UV CD) in the presence of different concentrations of arginine have been fit to a two-state model (eq 5), and the parameters obtained are listed in Table 1. Since the fluorescence data deviate from two-state behavior, they were not fitted. Both ΔG° and m increase with arginine concentration, indicating the stabilization of the secondary structure by arginine.

Fluorescence Correlation Spectroscopy (FCS) of Labeled BSA. While the frequency of application of FCS to biophysics, biochemistry, and cellular biology has been increasing significantly, a number of artifacts have been noted recently. It has been noted recently that the observation volume may deviate from three-dimensional Gaussian approximation at large pinhole diameters, leading to erroneous components (*29*). The effect of optical saturation and its effects on the autocorrelation function and the measured diffusion coefficients have been described recently (*30, 31*). Figure 4 shows the autocorrelation functions obtained from Alexa488Maleimide at attenuated powers of 1, 5, and 10%. The correlation functions were fit to a model containing a single diffusing species (eq 1), and the residual distributions are shown in Figure 4. The variation of the count per particle (CPP) with laser power is shown in the inset of Figure 4, which indicates a linear increase in CPP at lower powers. At higher powers, CPP values saturate presumably because of optical saturation and enhanced triplet effects. The residual distribution of the fit at a low laser power (lp1% in Figure 4) has been found to be random. At higher powers (for example, 10% in Figure 4), correlation function does not fit well to eq 1, resulting in nonrandom residual distribution (Figure 4).

Figure 5a shows a typical autocorrelation function obtained by FCS with Alexa488Maleimide-labeled BSA in phosphate buffer. The laser power was kept at 1% attenuation, which falls at the linear region of Figure 4. The data were fit successfully to a model containing a single diffusing

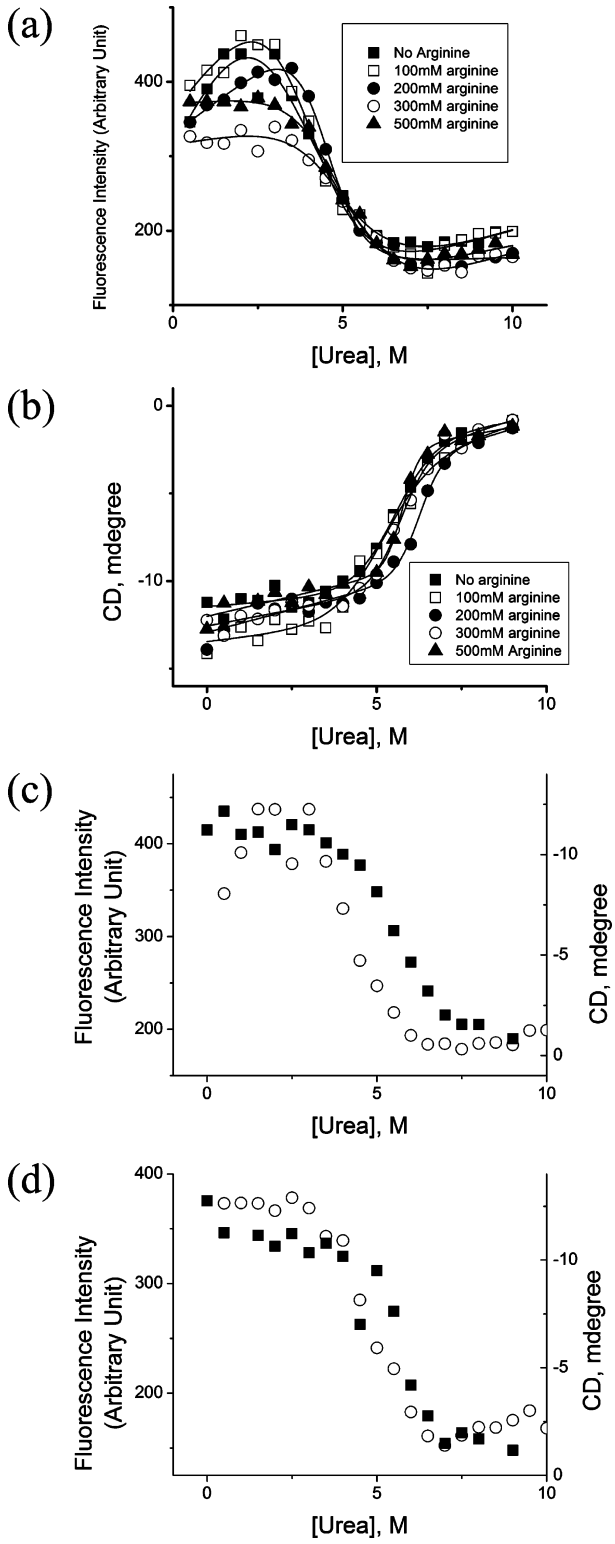

FIGURE 3: Urea-induced unfolding transitions of BSA in the presence of different concentrations of arginine monitored by (a) steady state fluorescence emission at 340 nm and (b) far-UV CD at 222 nm. Arginine concentrations are shown in the figures. Comparisons between the unfolding transitions probed by steady state fluorescence emission at 340 nm (○) and far-UV CD at 222 nm (■) are shown (c) in the absence of arginine and (d) in the presence of 500 mM arginine. All the experiments were conducted in the presence of 20 mM sodium phosphate buffer (pH 7.5) at room temperature. The solid line through the CD data in panel b is the fit to a typical two-state unfolding transition (eq 5). The fit line shown in the florescence data in panel a is for the purpose of presentation only, and these data were not used to calculate any thermodynamic parameters.

Table 1: Values of $\Delta G°$, m, and the Midpoints Obtained from the Unfolding Transitions Monitored by Far-UV CD in the Presence of Different Concentrations of Arginine[a]

[arginine] (mM)	$\Delta G°$ (kcal/mol)	m[b] (kcal mol^{-1} M^{-1})	midpoint (M)
0	5.2	−1	5.2
100	4.1	−0.8	5.1
200	10	−1.6	6.3
300	8	−1.3	6.2
500	15	−2.6	5.8

[a] Experiments were conducted in 20 mM phosphate buffer (pH 7.5) at room temperature. [b] Slope of the unfolding curve assuming a two-state model.

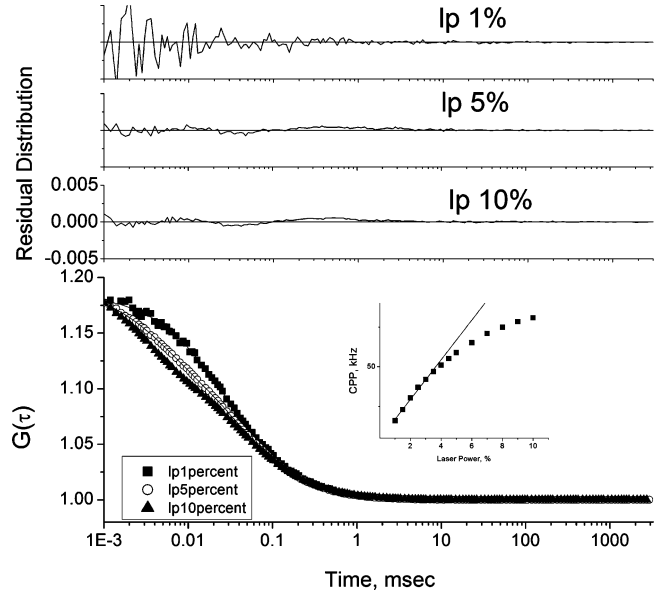

FIGURE 4: Normalized autocorrelation functions obtained from the FCS experiments with Alexa488Maleimide in the presence of different laser powers. The residual distributions obtained from the data fit to eq 1 are also shown. The inset shows the values of count per particles in kilohertz with power. A straight line simulated using the initial data points is drawn to estimate the deviation from the ideal straight-line behavior at higher powers. Nonrandomness in the residual distributions in the presence of a high laser power is also indicative of the nonideal nature of the observation volume. All the experiments were conducted at room temperature using 50−100 nM Alexa488Maleimide in the presence of 20 mM sodium phosphate buffer (pH 7.5).

component with a τ_D of 153 μs, and the goodness of the fit was checked by random residual distribution. Addition of a second component did not improve the fit. The diffusion coefficient (D) of the protein was calculated from the value of τ_D using eq 2, and the calculated value (0.6×10^{-11} m^2/s) matches well the published result of 0.51×10^{-11} m^2/s (*32*). The value of D was used to calculate the hydrodynamic radius (r_H) of BSA using the Stokes−Einstein formulation, and the calculated value (36 Å) agrees with the published results (*33*). Moreover, from the crystal structure (*34*), the volume of HSA is 192000 Å^3 and the hydrodynamic radius obtained from the crystal structure (36 Å) matches well with the radius calculated from the FCS data. The correlation data were further analyzed using the maximum entropy method (MEM) recently developed by Sengupta et al. (*28*). The maximum entropy distribution of Alexa488Maleimide-labeled BSA is shown in Figure 5b. A single component with the peak at 161 μs was observed which matches well with the τ_D value obtained by the conventional method (153

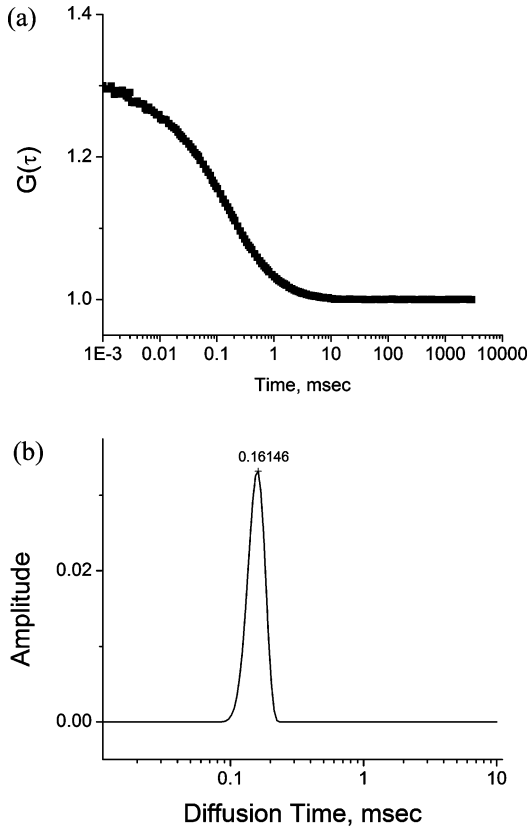

FIGURE 5: FCS data of Alexa488Maleimide-labeled BSA. (a) Normalized autocorrelation function and its fit using eq 1. (b) MEM profile of the same data. MEM analysis were performed using MEMFCS algorithm developed by Sengupta et al. (*28*). Experimental conditions are the same as those described in the legend of Figure 4.

Table 2: Values of τ_D, D, and r_H of Labeled BSA under Different Solution Conditions[a]

	τ_D (μs)	r (Å)
BSA (pH 7.5)	153	36
BSA in the presence of 500 mM arginine (pH 7.5)	126	30
BSA (pH 2)	223	53
BSA in the presence of 4.5 M urea (pH 7.5)	200	47
BSA in the presence of 8 M urea (pH 7.5)	290	68
unfolded BSA in 8 M urea and 500 mM arginine (pH 7.5)	263	63

[a] FCS experiments were performed at room temperature. All data are corrected for viscosity and solution refractive index change.

μs). Table 2 shows the diffusion time values and the calculated radius of BSA under different solution conditions.

The correlation function observed for the labeled protein in the presence of 500 mM arginine was fit to a model containing a single diffusing species with a τ_D of 126 μs. The calculated r_H of the protein in the presence of 500 mM arginine (30 Å) indicates a substantial decrease in the radius of the protein. While the reason for this apparent decrease in r_H in the presence of arginine is unknown, one possible hypothesis could be the change in hydration by arginine. We are planning to test this by NMR using a smaller protein. A recent sedimentation experiment with α-crystallin through a 10 to 40% glycerol gradient has shown an apparent decrease in the molecular mass to ~360 kDa in the presence of 300 mM arginine (compared to ~700 kDa in the absence of arginine) (*35*).

At pH 2, the values of τ_D and r_H increase to 225 μs and 53 Å, respectively. A recent FCS study on intestinal fatty acid binding protein shows a 33% increase in r_H at pH 2 as a result of partial unfolding (*14*). Formation of partially folded states and/or molten globule intermediates at low pH has been well-documented for a number of different proteins.

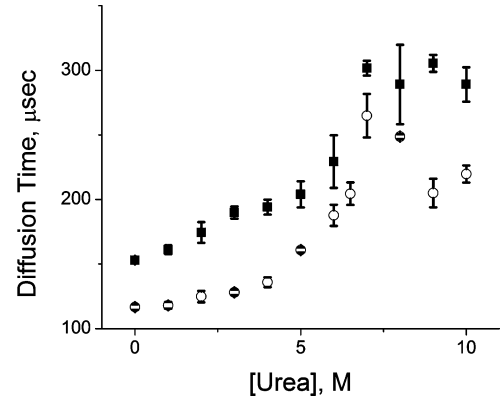

FIGURE 6: Urea-induced unfolding transitions of Alexa488Maleimide-labeled BSA in the absence (■) and presence (○) of 500 mM arginine. Autocorrelation functions were analyzed using the MEM. Diffusion time values, after normalization with experimental data for the free dye obtained at each urea concentration (*15*), were plotted with urea concentration. Experimental conditions are the same as those described in the legend of Figure 4.

Effects of Arginine on the Equilibrium Unfolding Transition of BSA Monitored by Fluorescence Correlation Spectroscopy. Urea-induced unfolding of BSA studied by steady state fluorescence and far-UV CD indicates formation of a pretransition intermediate state. This intermediate is characterized by a significant change in the aromatic region of the protein without any change in the secondary structure (Figure 3c). The presence of arginine inhibits formation of that pretransition intermediate, and the unfolding transitions probed by fluorescence and far-UV CD are superimposable (Figure 3d). To obtain further insight into the pretransition intermediate of BSA, we have followed the unfolding transitions of the protein in the absence and presence of arginine by using FCS. The correlation functions at different urea concentrations were fit to a single diffusion component. Data analysis by the conventional and maximum entropy method (MEM) yields identical results.

Figure 6 shows the variation of τ_D with urea concentration in the absence and presence of 500 mM arginine. The urea-induced unfolding transition, in the absence of arginine, shows the presence of two distinct transitions. The first transition or the formation of the intermediate occurs below 5 M urea and is characterized by an ~25% increase in τ_D. The second transition occurs between 5 and 8 M urea and is characterized a large increase in τ_D. The second transition coincides well with the unfolding of the secondary structure of BSA probed by far-UV CD (Figure 3d). The hydrodynamic radius of the protein in the intermediate state (in the presence of 4.5 M urea) was calculated to be 47 Å. In the presence of 8 M urea, when the protein is expected to be completely unfolded, r_H increases to 71 Å. In the presence of 500 mM arginine, τ_D increases cooperatively with urea concentration and no intermediate is detected.

Panels a and b of Figure 7 show the effect of 500 mM arginine on the maximum entropy distribution profiles of Alexa-labeled BSA in the presence of different urea concentrations. In the absence of arginine (Figure 6a), the MEM

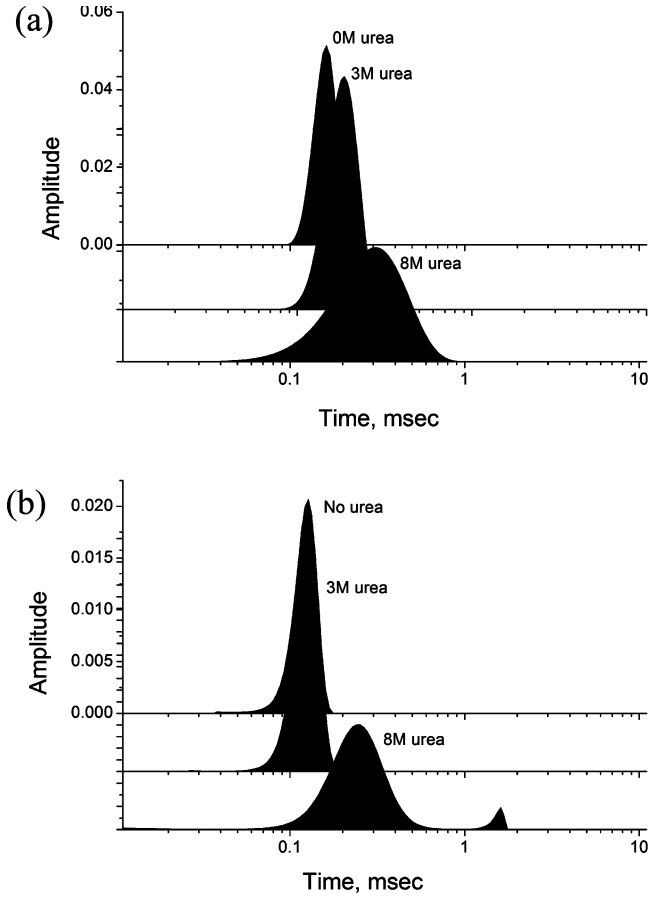

FIGURE 7: Variation of MEM profiles with urea concentration in the absence (a) and presence (b) of 500 mM arginine. Experimental conditions are the same as those described in the legend of Figure 4.

distribution shifts gradually to higher τ_D values at low urea concentrations. A second phase of shift in the MEM distribution occurs after 5 M urea, leading to the unfolding of the protein. In the presence of arginine, on the other hand, the MEM distribution does not change initially up to 4 M; a single phase of a large shift in the MEM distribution occurs beyond a urea concentration of 4 M.

DISCUSSION

We have used a number of analytical techniques like analytical ultracentrifugation, dynamic light scattering, and native gel electrophoresis to show that the addition of arginine inhibits the heat-induced aggregation of BSA. The importance of using orthogonal techniques like analytical ultracentrifugation and dynamic light scattering to detect, quantify, and characterize protein aggregation has been discussed recently (*36, 37*). Analytical ultracentrifugation is particularly useful as an analytical tool for accurately estimating the concentration of aggregates as it does not need use of any interfering column or matrix interaction (like size exclusion chromatography); it is sensitive and extremely accurate (*38*−*41*). Dynamic light scattering, on the other hand, is less sensitive but provides useful information at different protein concentrations (*42, 43*). This study as well as previous experiments has shown the importance of arginine as an additive in increasing the refolding yield and suppressing the aggregation of a number of protein systems (*3, 4, 44, 45*).

Scheme 1: Effect of Arginine on the Equilibrium Unfolding of BSA

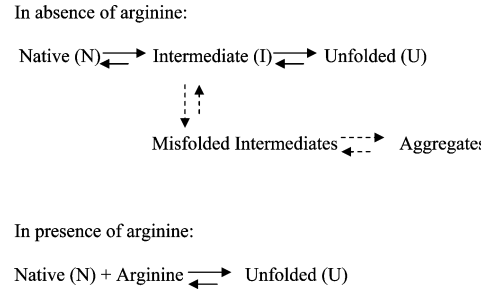

We show further that the addition of 500 mM arginine does not change the secondary structure of the protein significantly. We have seen a small change in the near-UV CD and in steady state fluorescence (data not shown), suggesting that while arginine may have influence on the aromatic region of BSA, its binding to protein should be weak. Similar observation has been reported by Ou et al. in their study on rabbit muscle creatine kinase (*43*).

We have studied unfolding transitions of BSA in the presence of arginine by using a number of different biophysical techniques, including steady state fluorescence, far-UV CD, and FCS. According to the data presented in this study, the effect of arginine on the unfolding transition of BSA can be modeled as shown in Scheme 1.

Intermediate I is partially unfolded with mostly intact secondary structure. The r_H of the intermediate is ~25% larger compared to that in the native state (Table 2). An intermediate with a similar r_H has been found to form at pH 2 (Table 2). The unfolded state (U) is extended with a significantly larger r_H. In the presence of 500 mM arginine, intermediate I is not populated in the unfolding pathway of BSA which may be important for arginine's role in inhibiting protein aggregation.

The data presented here show interesting similarity and dissimilarity with those of other osmolytes. The free energy of unfolding, $\Delta G°$, has been found to increase with arginine concentration (Table 1), indicating the stabilization of the protein by arginine. Similar results have been observed with heat-induced denaturation of BSA probed by differential scanning calorimmetry (K. Chattopadhyay, unpublished data). An increase in $\Delta G°$ can be interpreted in the following way. First, arginine either stabilizes the folded state or destabilizes the unfolded state of the protein. Alternatively, even if arginine destabilizes the folded state, it should also destabilize the unfolded state and the extent of destabilization of the unfolded states should be greater. The destabilization of the unfolded states relative to the native states of a protein by stabilizing osmolytes has been observed by Arakawa and Timasheff (*46*) and others (*47*). Ordering of water molecule by osmolyte as described by Zou et al. (*48*) would lead to an unfavorable transfer of free energy of the peptide backbone from water to osmolyte, resulting in the destabilization of relatively more extended unfolded states.

The increase in the parameter *m*, on the other hand, suggests an increase in ΔASA (ΔASA being the change in the solvent accessibility upon unfolding) as defined by Myers et al. (*49*) by arginine. This is not expected as Qu et al. have shown before that stabilizing osmolytes act on the protein backbone to contract the unfolded states of a protein (*50*).

Our preliminary FCS data on the addition of 500 mM arginine to the unfolded BSA at 8 M urea result in an ~8% decrease in τ_D (Table 2), which shows that arginine does indeed contract the unfolded states. Contraction of the unfolded state by the osmolytes should decrease ΔASA, and hence, the value of *m* should also be decreased. The increase in *m* by arginine can be explained by our FCS data, which suggest a larger contraction of the native state of BSA [~20% decrease in the diffusion time of BSA by arginine (Table 2)]. However, it should be noted that the presence of an intermediate in the unfolding pathway would also decrease the parameter *m* (*51*). Both the effects may contribute together to the overall increase in cooperativity in the presence of arginine.

The native state contraction of the protein by arginine, while surprising, has been observed before (*35*). Guanidine hydrochloride, which is similar to arginine in structure, was also found to form a contracted intermediate state at its low concentration (*52*). Unlike other stabilizing osmolytes, which interact exclusively on the protein backbone at the unfolded states, arginine has been shown to interact with the aromatic side chains and bind efficiently to either the native state or the partially folded intermediates of a protein (*53, 54*), which is similar to the action of a destabilizing agent like urea or guanidine hydrochloride.

Formation of intermediate states in the protein folding pathway has been studied extensively. While the presence of an on-pathway intermediate can be productive toward efficient folding of a protein, non-native contact formation could result in aggregation. The early occurrence of nativelike tertiary interactions within a molten globule intermediate of the helical domain of human lactalbumin has been shown by Peng et al. (*55*). The initial onset of the native tertiary fold in the molten globule is expected to lead to significant reduction in the conformational space to be searched by the protein which would then be followed by the consolidation of the side chain packing (*55, 56*). Non-native contact formation, on the other hand, would result in the accumulation of stable compact intermediates as shown recently by Rea et al. (*57*). These intermediates have undesirable consequences and must be unfolded before proper folding can occur (*57*). Several recent studies have shown the presence of an extensive structural network in the unfolded states of a protein (*15, 16, 58*), and the nature of contact formation early in the unfolded states may be crucial in determining the nature of the intermediate states.

It would be interesting to relate arginine's ability to suppress aggregation and its role in blocking the intermediate states of BSA. Another important question which remains to be addressed is whether these effects of arginine are protein specific or can be generalized to other protein systems. It may be possible that arginine interacts early in the unfolded states and influences the nature of contact formation. Alternatively, arginine may also bind to the hydrophobic clusters present in the unfolded states. A particularly interesting choice of a protein system would be to understand some of these issues, which folds downhill at the speed limit (*59*). It has been shown recently by Chattopadhyay et al. that FCS in concert with fluorescence self-quenching can be used efficiently to monitor rapid contact formation in the chemically unfolded state of a protein (*16*), and this technique can be useful in verifying this hypothesis.

In this study, we show that arginine can behave both as a stabilizing and as a destabilizing osmolyte. It contracts the unfolded state of a protein, which is typical of a protecting osmolyte like sucrose or betaine (*52*). On the other hand, arginine like guanidine hydrochloride or urea can bind effectively to the partially folded intermediates. The fine-tuning of both the stabilizing and destabilizing properties of arginine makes it a potent agent for inhibiting protein aggregation. Effort is being spent in our laboratory to design a series of experimental conditions by varying pH and buffer conditions and by employing a number of different proteins and their site-directed mutants to modulate the stabilizing and destabilizing roles of this interesting amino acid.

ACKNOWLEDGMENT

We thank Dr. D. Bhattacharya, Dr. G. Sureshkumar, and Prof. S. Roy (Indian Institute of Chemical Biology) for allowing us to use their laboratory facilities. We also thank Prof. S. Maiti of the Tata Institute of Fundamental Research for kindly providing us the MEMFCS software. K.C. thanks Prof. Carl Frieden (Washington University School of Medicine, St. Louis, MO) for his critical comments on the manuscript.

REFERENCES

1. Andya, J. D., Hsu, C. C., and Shire, S. J. (2003) Mechanisms of aggregate formation and carbohydrate excipient stabilization of lyophilized humanized monoclonal antibody formulations. *AAPS PharmSci 5*, E10.
2. Andya, J. D., Maa, Y. F., Costantino, H. R., Nguyen, P. A., Dasovich, N., Sweeney, T. D., Hsu, C. C., and Shire, S. J. (1999) The effect of formulation excipients on protein stability and aerosol performance of spray-dried powders of a recombinant humanized anti-IgE monoclonal antibody. *Pharm. Res. 16*, 350–358.
3. Arakawa, T., Ejima, D., Tsumoto, K., Obeyama, N., Tanaka, Y., Kita, Y., and Timasheff, S. N. (2007) Suppression of protein interactions by arginine: A proposed mechanism of the arginine effects. *Biophys. Chem. 127*, 1–8.
4. Arakawa, T., Kita, Y., Ejima, D., Tsumoto, K., and Fukada, H. (2006) Aggregation suppression of proteins by arginine during thermal unfolding. *Protein Pept. Lett. 13*, 921–927.
5. Arakawa, T., Tsumoto, K., Nagase, K., and Ejima, D. (2007) The effects of arginine on protein binding and elution in hydrophobic interaction and ion-exchange chromatography. *Protein Expression Purif. 54*, 110–116.
6. Arakawa, T., Ejima, D., Tsumoto, K., Ishibashi, M., and Tokunaga, M. (2007) Improved performance of column chromatography by arginine: Dye-affinity chromatography. *Protein Expression Purif. 52*, 410–414.
7. Yancey, H. P., Clark, E. M., Hand, C. S., Bowlus, D. R., and Sumero, N. G. (1982) Living with Water Stress: Evolution of Osmolyte System. *Science 217*, 1214–1222.
8. Baynes, B. M., Wang, D. I. C., and Trout, B. L. (2005) Role of arginine in the stabilization of proteins against aggregation. *Biochemistry 44*, 4919–4925.
9. Qiang Xie, T. g., Lu, J., and Zhou, H.-M. (2004) The guanidine like effects of arginine on aminoacylase and salt-induced molten globule state. *Int. J. Biochem. Cell Biol. 36*, 296–306.
10. Elson, E. L. (1985) Fluorescence correlation spectroscopy and photobleaching recovery. *Annu. Rev. Phys. Chem. 36*, 379–406.
11. Hess, S. T., Huang, S., Heikal, A. A., and Webb, W. W. (2002) Biological and chemical applications of fluorescence correlation spectroscopy: A review. *Biochemistry 41*, 697–705.
12. Schwille, P., Korlach, J., and Webb, W. W. (1999) Fluorescence correlation spectroscopy with single-molecule sensitivity on cell and model membranes. *Cytometry 36*, 176–182.
13. Webb, W. W. (1976) Applications of fluorescence correlation spectroscopy. *Q. Rev. Biophys. 9*, 49–68.
14. Chattopadhyay, K., Saffarian, S., Elson, E. L., and Frieden, C. (2002) Measurement of microsecond dynamic motion in the

intestinal fatty acid binding protein by using fluorescence correlation spectroscopy. *Proc. Natl. Acad. Sci. U.S.A. 99*, 14171–14176.
15. Chattopadhyay, K., Saffarian, S., Elson, E. L., and Frieden, C. (2005) Measuring unfolding of proteins in the presence of denaturant using fluorescence correlation spectroscopy. *Biophys. J. 88*, 1413–1422.
16. Chattopadhyay, K., Elson, E. L., and Frieden, C. (2005) The kinetics of conformational fluctuations in an unfolded protein measured by fluorescence methods. *Proc. Natl. Acad. Sci. U.S.A. 102*, 2385–2389.
17. Garai, K., Sureka, R., and Maiti, S. (2007) Detecting amyloid-β aggregation with fiber-based fluorescence correlation spectroscopy. *Biophys. J. 92*, L55–L57.
18. Haupts, U., Maiti, S., Schwille, P., and Webb, W. W. (1998) Dynamics of fluorescence fluctuations in green fluorescent protein observed by fluorescence correlation spectroscopy. *Proc. Natl. Acad. Sci. U.S.A. 95*, 13573–13578.
19. Petersen, N. O. (1984) Diffusion and aggregation in biological membranes. *Can. J. Biochem. Cell Biol. 62*, 1158–1166.
20. Schwille, P., Maiti, S., and Webb, W. W. (1999) Molecular dynamics in living cells observed by fluorescence correlation spectroscopy with one- and two-photon excitation. *Biophys. J. 77*, 2251–2265.
21. Schwille, P., Kummer, S., Heikal, A. A., Moerner, W. E., and Webb, W. W. (2000) Fluorescence correlation spectroscopy reveals fast optical excitation-driven intramolecular dynamics of yellow fluorescent proteins. *Proc. Natl. Acad. Sci. U.S.A. 97*, 151–156.
22. Arakawa, T., and Kita, Y. (2000) Protection of bovine serum albumin from aggregation by Tween 80. *J. Pharm. Sci. 89*, 646–651.
23. Dockal, M., Carter, D. C., and Ruker, F. (2000) Conformational transitions of the three recombinant domains of human serum albumin depending on pH. *J. Biol. Chem. 275*, 3042–3050.
24. Kumar, Y., Tayyab, S., and Muzammil, S. (2004) Molten-globule like partially folded states of human serum albumin induced by fluoro and alkyl alcohols at low pH. *Arch. Biochem. Biophys. 426*, 3–10.
25. Militello, V., Casarino, C., Emanuele, A., Giostra, A., Pullara, F., and Leone, M. (2004) Aggregation kinetics of bovine serum albumin studied by FTIR spectroscopy and light scattering. *Biophys. Chem. 107*, 175–187.
26. Brown, P., and Schuck, P. (2006) Macromolecular size-and-shape distributions by sedimentation velocity analytical ultracentrifugation. *Biophys. J. 90*, 4651–4661.
27. Lakowicz, J. R. (1983) *Principles of Fluorescence Spectroscopy*, Plenum Press, New York.
28. Sengupta, P., Garai, K., Balaji, J., Periasamy, N., and Maiti, S. (2003) Measuring size distribution in highly heterogeneous systems with fluorescence correlation spectroscopy. *Biophys. J. 84*, 1977–1984.
29. Hess, S. T., and Webb, W. W. (2002) Focal volume optics and experimental artifacts in confocal fluorescence correlation spectroscopy. *Biophys. J. 83*, 2300–2317.
30. Gregor, I., Patra, D., and Enderlein, J. (2005) Optical saturation in fluorescence correlation spectroscopy under continous wave and pulsed excitation. *ChemPhysChem 6*, 164–170.
31. Mutze, J., Petrasek, Z., and Schwille, P. (2007) Independence of Maximum Single Molecule Fluorescence Count Rate on the Temporal and Spectral Laser Pulse Width in Two-Photon FCS. *J. Fluoresc. 17*, 805–810.
32. Krouglova, T., Vercammen, J., and Engelborghs, Y. (2004) Correct Diffusion Coefficients of Proteins in Fluorescence Correlation Spectroscopy. Application to Tubulin Oligomers Induced by Mg21 and Paclitaxel. *Biophys. J. l87*, 2635–2646.
33. Johnson, E. M., Berk, D. A., Jain, R. K., and Deen, W. M. (1996) Hindered Diffusion in Agarose Gels: Test of Effective Medium Model. *Biophys. J. 70*, 1017–1026.
34. Sugio, S., Kashima, A., Mochizuki, M., Noda, M., and Kobayashi, K. (1999) Crystal structure of human serum albumin at 2.5 Å resolution. *Protein Eng. 12*, 439–446.
35. Srinivas, V., Raman, B., Rao, K. S., Ramakrishna, T., and Rao, C. M. (2003) Structural perturbation and enhancement of the chaperon-like activity of α-crystallin by arginine hydrochloride. *Protein Sci. 12*, 1262–1270.
36. Gabrielson, J. P., Brader, M. L., Pekar, A. H., Mathis, K. B., Winter, G., Carpenter, J. F., and Randolph, T. W. (2007) Quantitation of aggregate levels in a recombinant humanized monoclonal antibody formulation by size-exclusion chromatography, asymmetrical flow field flow fractionation, and sedimentation velocity. *J. Pharm. Sci. 96*, 268–279.
37. Philo, J. S. (2006) Is any measurement method optimal for all aggregate sizes and types. *AAPS J. 8*, E564–E571.
38. Arakawa, T., and Philo, J. S. (1999) [Applications of analytical ultracentrifuge to molecular biology and pharmaceutical science]. *Yakugaku Zasshi 119*, 597–611.
39. Berkowitz, S. A. (2006) Role of analytical ultracentrifugation in assessing the aggregation of protein biopharmaceuticals. *AAPS J. 8*, E590–E605.
40. Liu, J., Andya, J. D., and Shire, S. J. (2006) A critical review of analytical ultracentrifugation and field flow fractionation methods for measuring protein aggregation. *AAPS J. 8*, E580–E589.
41. Pekar, A., and Sukumar, M. (2007) Quantitation of aggregates in therapeutic proteins using sedimentation velocity analytical ultracentrifugation: Practical considerations that affect precision and accuracy. *Anal. Biochem. 367*, 225–237.
42. Oliva, A., Llabres, M., and Farina, J. B. (2004) Applications of multi-angle laser light-scattering detection in the analysis of peptides and proteins. *Curr. Drug Discovery Technol. 1*, 229–242.
43. Ou, W., R.-S. W., Lu, J., and Zhou, H.-M. (2003) Effects of arginine on rabbit muscle creatine kinase and salt-induced molten globule-like state. *Biochim. Biophys. Acta 1652*, 7–16.
44. Arakawa, T., Kita, Y., and Koyama, A. H. (2008) Solubility enhancement of gluten and organic compounds by arginine. *Int. J. Pharm. 355*, 220–223.
45. Bajorunaite, E., Sereikaite, J., and Bumelis, V. A. (2007) L-Arginine suppresses aggregation of recombinant growth hormones in refolding process from *E. coli* inclusion bodies. *Protein J. 26*, 547–555.
46. Arakawa, T., Bhat, R., and Timasheff, S. N. (1990) Preferential interactions determine protein solubility in three-component solutions: The $MgCl_2$ system. *Biochemistry 29*, 1914–1923.
47. Mandal, A. K., Samaddar, S., Banerjee, R., Lahiri, S., Bhattacharyya, A., and Roy, S. (2003) Glutamate counteracts the denaturing effect of urea through its effect on the denatured state. *J. Biol. Chem. 278*, 36077–36084.
48. Zou, Q., Bennion, B. J., Daggett, V., and Murphy, K. P. (2002) The molecular mechanism of stabilization of proteins by TMAO and its ability to counteract the effects of urea. *J. Am. Chem. Soc. 124*, 1192–1202.
49. Myers, J. K., Pace, C. N., and Scholtz, J. M. (1995) Denaturant m values and heat capacity changes: Relation to changes in accessible surface areas of protein unfolding. *Protein Sci. 4*, 2138–2148.
50. Qu, Y., Bolen, C. L., and Bolen, D. W. (1998) Osmolyte-driven contraction of a random coil protein. *Proc. Natl. Acad. Sci. U.S.A. 95*, 9268–9273.
51. Pace, C. N. (1986) Determination and analysis of urea and guanidine hydrochloride denaturation curves. *Methods Enzymol. 131*, 266–280.
52. Nidhi Shukla, A. n. B., Aliverti, A., Zanetti, G., and Bhakuni, V. (2005) Guanidinium chloride- and urea-induced unfolding of FprA, a mycobacterium NADPH-ferredoxin reductase stabilization of an apo-protein by GdmCl. *FEBS J. 272*, 2216–2224.
53. Das, U., Hariprasad, G., Ethayathulla, A. S., Manral, P., Das, T. K., Pasha, S., Mann, A., Ganguli, M., Verma, A. K., Bhat, R., Chandrayan, S. K., Ahmed, S., Sharma, S., Kaur, P., Singh, T. P., and Srinivasan, A. (2007) Inhibition of protein aggregation: Supramolecular assemblies of arginine hold the key. *PLoS ONE 2*, e1176.
54. Ishibashi, M., Tsumoto, K., Ejima, D., Arakawa, T., and Tokunaga, M. (2005) Characterization of arginine as a solvent additive: A halophilic enzyme as a model protein. *Protein Pept. Lett. 12*, 649–653.
55. Peng, Z. H., and Kim, P. S. (1994) A Protein Dissection Study of a Molten Globule. *Biochemistry 33*, 2136–2141.
56. Chattopadhyay, K., Zhong, S., Yeh, S.-R., Rousseau, D. L., and Frieden, C. (2002) The intestinal fatty acid binding protein: The role of turns in fast and slow folding processes. *Biochemistry 41*, 4040–4047.
57. Rea, A. M., Simpson, E. R., Meldrum, J. K., Williams, H. E. L., and Searle, M. S. (2008) Aromatic Residues Engineered into the β-Turn Nucleation Site of Ubiquitin Lead to a Complex Folding Landscape, Non-Native Side-Chain Interactions, and Kinetic Traps. *Biochemistry 47*, 12910–12922.
58. Dill, K. A. S. D. (1991) Denatured states of proteins. *Annu. Rev. Biochem. 60*, 795–825.
59. Kubelka, J. H., Jr., and Eaton, W. A. (2004) The protein folding 'speed limit'. *Curr. Opin. Struct. Biol. 14*, 76–88.

BI802065J